Size-Selected Infrared Predissociation Spectroscopy of Neutral and Cationic Formamide−Water Clusters: Stepwise Growth of Hydrated Structures and Intracluster Hydrogen Transfer Induced by Vacuum-Ultraviolet Photoionization

Daichi Sakai, Yoshiyuki Matsuda,* Masaki Hachiya, Mayumi Mori, Asuka Fujii, and Naohiko Mikami*

Department of Chemistry, Graduate School of Science, Tohoku University, Aramaki-Aoba, Aoba-ku, Sendai 980-8578, Japan

Received: January 25, 2008; Revised Manuscript Received: March 12, 2008

Vibrational spectroscopy of size-selected formamide−water clusters, FA−$(H_2O)_n$, $n = 1-4$, prepared in a supersonic jet is performed with vacuum-ultraviolet−ionization detected−infrared predissociation spectroscopy (VUV-ID-IRPDS). The cluster structures are determined through comparisons of the observed IR spectra with theoretical calculations at the MP2/6-31++G** level. The FA−$(H_2O)_n$, $n = 1-3$, clusters have ring-type structures, where water molecules act as both single donor and single acceptor in the hydrogen-bond network between the amino and carbonyl groups of FA. For FA−$(H_2O)_4$, on the other hand, the absence of the free NH stretching vibration indicates formation of a double ring type structure, where two NH bonds of the amino group and the carbonyl oxygen of FA form hydrogen bonds with water molecules. An infrared spectrum of the formamide−water cluster cation, $[FA-H_2O]^+$, is also observed with infrared predissociation spectroscopy of vacuum-ultraviolet-pumped ion (IRPDS-VUV-PI). No band is observed for the free OH stretches of neutral water. This shows $[FA-H_2O]^+$ has such a structure that one of the hydrogen atoms of the water moiety is transferred to the carbonyl oxygen of FA^+.

I. Introduction

Gas-phase clusters of organic and biological molecules are regarded as simplified microscopic models of their solvation phenomena in bulk systems. Size-selected cluster approach with various laser spectroscopic techniques enables us to study solvated structures, solute−solvent interactions, and solvation effects on molecular properties at the microscopic level. Clusters of various molecules with water, alcohol, ammonia, and so on have been extensively investigated for their geometric structures in terms of intermolecular interactions such as the dispersion force, electrostatic interaction, and hydrogen bond (H-bond).[1–6]

Formamide (FA) is the simplest molecule having an amide group, and its structure corresponds to the N-terminal end of polypeptides. The solvated cluster of FA is a prototype for solvation structures of peptides and the intermolecular interactions between the amide group and surrounding solvent molecules. The protonated and anionic clusters of FA have been investigated by infrared (IR)[7,8] and photoelectron spectroscopies,[9,10] and theoretical calculations.[7,8,10–17] On the other hand, only a few spectroscopic investigations have been reported for neutral clusters of FA, in spite of their importance. This is due to the fact that size-selective spectroscopic techniques such as conventional IR−ultraviolet (UV) double resonance spectroscopy[1,3,5,6] are inapplicable to neutral clusters of FA, which have no suitable UV chromophore for the fluorescence or multiphoton ionization (MPI) detection. Only FA−H_2O, FA−CH_3OH, and $(FA)_2$ have exceptionally undergone spectroscopic investigations.[18–20] The structures of FA−H_2O and FA−CH_3OH have been experimentally determined by microwave spectroscopy.[18] Both clusters form the ring type structures, where two H-bonds are formed between the amide group of FA and the solvent molecule. Another minor structural isomer as well as the most stable ring type form was observed in the Ar-matrix experiment.[21] Schermann and co-workers observed the IR spectra of FA−H_2O and $(FA)_2$ in the molecular beam by IR dissociation/electron detachment spectroscopy based on their Rydberg electron-transfer (RET) technique.[19,20,22] However, systematic size-selected spectroscopic studies for FA−$(H_2O)_n$, $n > 1$, have never been reported, so far. The new methodology has been required for systematic spectroscopic investigation of the size-selected neutral clusters of FA.

For various cations of protic[23–25] and organic molecules[7,8,26] such as FA, only protonated clusters have ordinarily been investigated with spectroscopic methods. Since such protonated clusters are easily produced by various ionization methods such as electron impact, discharge, fast atom bombardment, chemical ionization, multiphoton ionization, and so on,[7,8,23–27] extensive studies on them have been reported with respect to their geometric structures, protonation process, and intermolecular interactions.[7,8,11–17,23–27] Chang and co-workers performed the IR predissociation spectroscopy and theoretical calculations for $H^+FA-(H_2O)_n$ and $H^+(FA)_n$ and revealed that the protonation to the carbonyl oxygen is more favorable than that to the amino nitrogen.[7,8] On the other hand, spectroscopic investigations for unprotonated cluster cations of FA have been hardly reported, because of difficulties of their production. Cluster cations of such protic molecules are generated only by vacuum-ultraviolet (VUV) one-photon ionization,[28] multiphoton ionization with a femtosecond laser,[29] and electron impact within a He droplet.[30]

Recently, several vibrational spectroscopic techniques based on VUV photoionization detection have been developed

* To whom correspondence should be addressed. Phone: +81-22-795-6573. Fax: +81-22-795-6785. E-mail: y-matsuda@mail.tains.tohoku.ac.jp (Y.M.); nmikami@mail.tains.tohoku.ac.jp (N.M.).

10.1021/jp800743b CCC: $40.75
Published on Web 07/08/2008

for bare molecules and neutral and cationic clusters.[31–35] Among them, we have developed a size-selected IR predissociation spectroscopic scheme for neutral clusters, which uses soft ionization by VUV one-photon absorption, and this scheme is called VUV−ionization detected−IR predissociation spectroscopy (VUV-ID-IRPDS).[34] In this spectroscopy, IR spectra of size-selected clusters can be observed by monitoring the cluster ion signal, which is due to the ionization without fragmentation by the VUV light. VUV-ID-IRPDS can be, in principle, applied to vibrational spectroscopic studies of any clusters with the size-selection. IR predissociation spectroscopy of VUV−pumped ion (IRPDS-VUV-PI)[34,36] has been also developed for vibrational spectroscopy of cluster cations. This method is applicable for vibrational spectroscopic studies of unstable cluster cations, which can be produced only by the VUV photoionization.

These two new techniques are suitable for vibrational spectroscopic investigations of neutral and cationic hydrated clusters of FA, respectively. In the present study, we applied VUV-ID-IRPDS to the observation of vibrational spectra of neutral FA−water clusters, FA−$(H_2O)_n$, $n = 1-4$. The spectroscopic scheme of VUV-ID-IRPDS is tested by the observations of IR spectra of size-selected FA−$(H_2O)_n$ clusters. The cluster structures are investigated by comparing the observed IR spectra with simulated ones on the basis of ab initio calculations at the MP2/6-31++G** level.

The IR spectrum of unprotonated formamide−water cation, $[FA-H_2O]^+$, is also observed with IRPDS-VUV-PI. The cluster structure and properties of $[FA-H_2O]^+$ are discussed by the observed IR spectra and the MP2 level calculations of the optimized structure, normal-mode frequencies, and atomic charges.

II. Experiment

VUV-ID-IRPDS and IRPDS-VUV-PI were used for observations of IR spectra of FA−$(H_2O)_n$, $n = 1-4$, and $[FA-H_2O]^+$, respectively.

The experimental setup of VUV-ID-IRPDS for neutral clusters was described in detail elsewhere.[34] Here, we briefly describe the spectroscopic principle and experimental setup. The neutral clusters produced by a supersonic jet expansion were softly ionized by VUV (118 nm) one-photon absorption. The ionized cluster signal intensities were monitored through size selection with a time-of-flight (TOF) mass spectrometer. The cluster cation signal in a particular mass channel is the measure of the population of the neutral cluster of the same size when the neutral clusters were ionized without fragmentation. The reduction of the cluster ion signal intensity was caused by predissociation following vibrational excitation of the neutral cluster induced by the IR light, which was introduced prior to the VUV light. By scanning the IR frequency, while monitoring the reduction of the size-selected ion signal intensities, the IR-dip spectra of the size-selected neutral clusters were measured.

IRPDS-VUV-PI for cluster cations can be performed with the same experimental setup as VUV-ID-IRPDS.[34] The only difference between these two methods is the incidence timing of the IR light. In IRPDS-VUV-PI, the IR light is delayed by ~15 ns from the VUV light. Jet-cooled neutral clusters were ionized with the VUV one-photon absorption, and their cation signal intensities were monitored through size-selection by the TOF mass spectrometer. With monitoring the cation signal intensities, IR predissociation spectroscopy of size-selected cluster cation was performed.

The 118 nm light was generated by the third harmonic generation of the 355 nm (THG) output of a Nd:YAG laser (Continuum Surelite-III) with a Xe−Ar (1:10) mixture at ~200 Torr in a gas cell, which is directly attached to a vacuum chamber. The IR light was generated by differential frequency generation of the 532 nm (SHG) output of an injection-seeded Nd:YAG laser (Continuum Powerlite 8010) and a dye laser (Continuum ND-6000) output (620−665 nm) with a $LiNbO_3$ crystal. The VUV and IR light pulses were coaxially introduced at the 15 mm down stream of the skimmed (by a skimmer of 2 mm diameter) supersonic molecular beam in the ionization region of the Wiley−McLaren type TOF mass spectrometer.

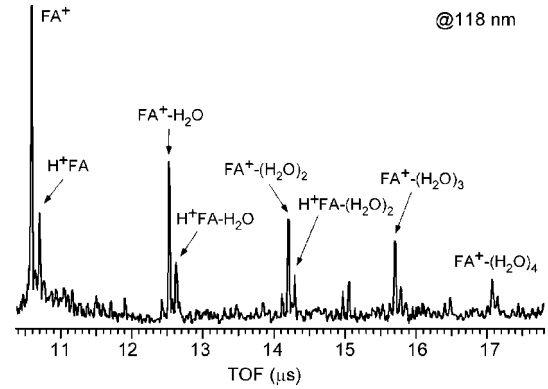

Figure 1. TOF mass spectrum of formamide and its water cluster cations observed by 118 nm one-photon ionization.

The formamide sample (>98.5%, Tokyo Chemical Industry Co., Ltd.) was used without further purification. It was supersonically expanded into the vacuum chamber through a pulsed nozzle with heating at ~323 K. Ar gas was used as the carrier gas.

Theoretical calculations for optimized structures, relative conformation energies, and vibrational frequencies of FA−$(H_2O)_n$ ($n = 1-4$) were carried out at the MP2 (second-order Møller-Plesset perturbation theory)/6-31++G** level with the Gaussian 03 program.[37] Calculations of $[FA-H_2O]^+$ were also obtained by the same level. Optimized structures are visualized with the MOLKEL program.[38]

III. Results

Figure 1 shows the TOF mass spectrum of FA and its water cluster cations, which are formed by the 118 nm (VUV) one-photon ionization of jet-cooled neutral clusters in the Ar expansion gas. Both series of the unprotonated and protonated FA−water cluster cations are observed, and the signal intensities of unprotonated cluster cations are larger than those of the protonated ones. The presence of unprotonated cluster cations implies the clusters are softly ionized with the VUV one-photon in comparison with other ionization techniques,[7,8,11] which only generate the protonated species.

Figure 2 presents the IR spectra of a neutral cluster of FA with water observed by monitoring the $[FA-H_2O]^+$ mass channel at the IR power of (a) ~0.5 and (b) ~0.25 mJ. Similarly, Figures 3–5 represent the IR spectra of neutral clusters by monitoring the $[FA-(H_2O)_2]^+$, $[FA-(H_2O)_3]^+$, and $[FA-(H_2O)_4]^+$ mass channels, respectively. Stick spectra in Figures 2–5 are calculated vibrational spectra obtained for the optimized structures at the MP2/6-31++G** level. The structures are shown in Figure 6–9, and they are discussed in section IV-2. Figure 10 shows the expanded spectra of the IR spectra in Figures 2–5 in the regions of (a) H-bonded NH and OH, (b) free NH, and (c) free OH stretching vibrations. The free OH stretching vibrational bands are

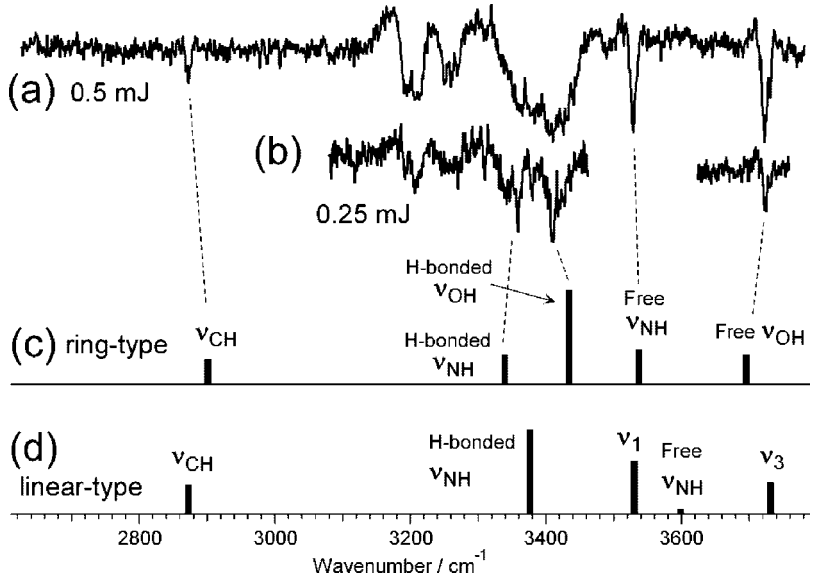

Figure 2. Infrared predissociation spectra of FA−H_2O observed by monitoring the $[FA-H_2O]^+$ signal with VUV−ionization detected−IR predissociation spectroscopy (VUV−ID−IRPDS) at the IR power of (a) ∼0.5 and (b) 0.25 mJ. (c, d) Calculated spectra for the optimized structures in Figure 6 at the MP2/6-31++G** level. The calculated spectra are scaled by 0.933.

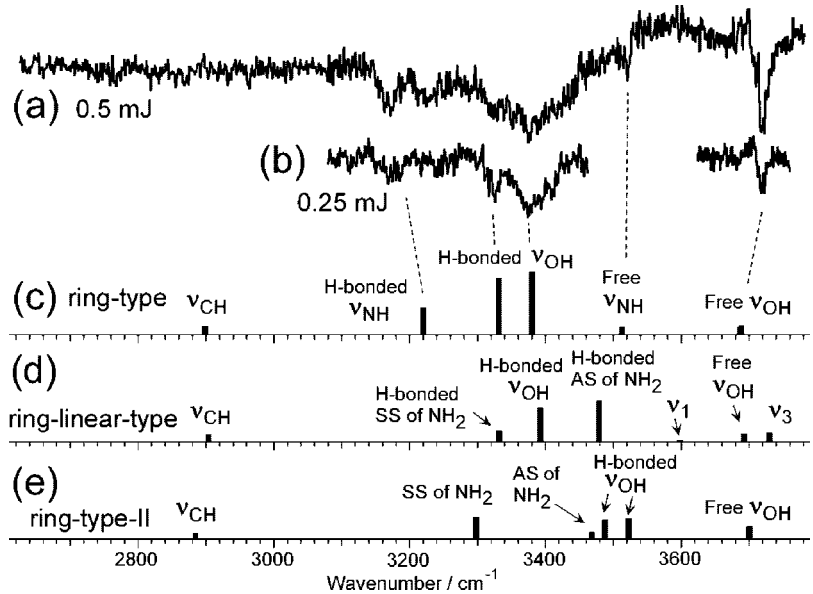

Figure 3. Infrared predissociation spectra of FA−$(H_2O)_2$ observed by monitoring the $[FA-(H_2O)_2]^+$ signal with VUV−ID−IRPDS at the IR power of (a) ∼0.5 and (b) 0.25 mJ. (c−e) Calculated spectra for the optimized structures in Figure 7 at the MP2/6-31++G** level. The calculated spectra are scaled by 0.933.

shifted to the lower frequency side with an increase of the cluster size. The peak position of the free NH stretching vibration also shows the lower frequency shift with the size (no band is observed in the free NH stretching vibrational region in $n = 4$). Thus, the spectral structures of the IR spectra observed for the different mass channels differ from each other. These spectral differences indicate that the IR spectra of size-selected neutral FA−$(H_2O)_n$ are successfully observed, and the size selectivity of VUV-ID-IRPDS is clearly demonstrated. The assignments of the spectral carriers for the IR spectra and observed bands are discussed in the Discussion.

The $[FA-H_2O]^+$ ion is generated by the 118 nm one-photon ionization, as shown in the mass spectrum in Figure 1. The IR spectrum of $[FA-H_2O]^+$ is observed with IRPDS-VUV-PI, where the IR light pulse is delayed by the VUV light pulse. Figure 11 presents the observed IR spectrum of $[FA-H_2O]^+$ and the stick spectra on the basis of the harmonic vibrational calculations for the optimized structures of $[FA-H_2O]^+$ at the MP2/6-31++G** level. The optimized structures are shown in Figure 12. Three intense bands in the region of 3250−3650 cm^{-1} and a weak band at 3028 cm^{-1} are observed. The latter can be assigned to the CH stretching vibration. No band appears in the range of 3650−3790 cm^{-1}, which is the characteristic region of ν_3 or free OH stretching vibration of neutral water. For FA−H_2O, the water moiety cannot be ionized by the 118 nm one-photon ionization, because the photon energy of 118 nm (10.5 eV) is much lower than the ionization energy of water (12.6 eV [39]). Therefore, $[FA-H_2O]^+$ is formed through ionization of the FA moiety of neutral FA−H_2O. No observation of the characteristic vibration of neutral water indicates the neutral form of water is not kept in the $[FA-H_2O]^+$ structure. The more details of the cluster structure of $[FA-H_2O]^+$ are discussed by

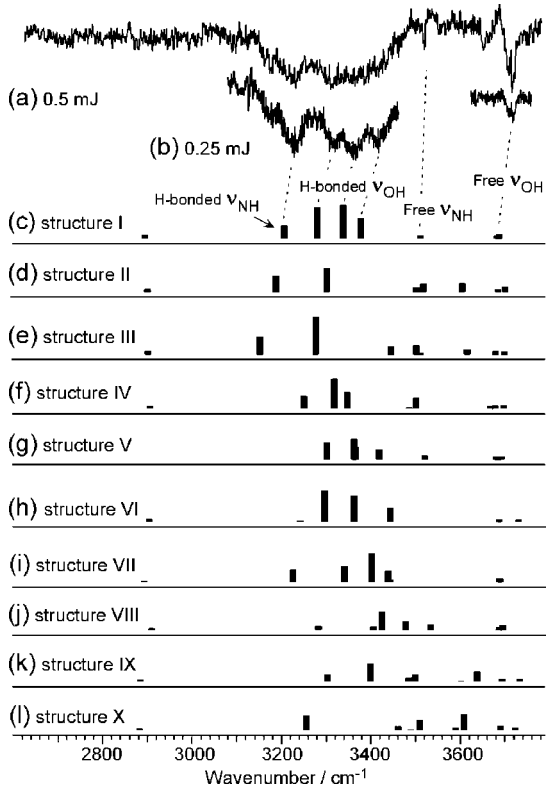

Figure 4. Infrared predissociation spectra of FA−$(H_2O)_3$ observed by monitoring the $[FA-(H_2O)_3]^+$ signal with VUV−ID−IRPDS at the IR power of (a) ∼0.5 and (b) 0.25 mJ. (c−l) Calculated spectra for the optimized structures in Figure 8 at the MP2/6-31++G** level. The calculated spectra are scaled by 0.933.

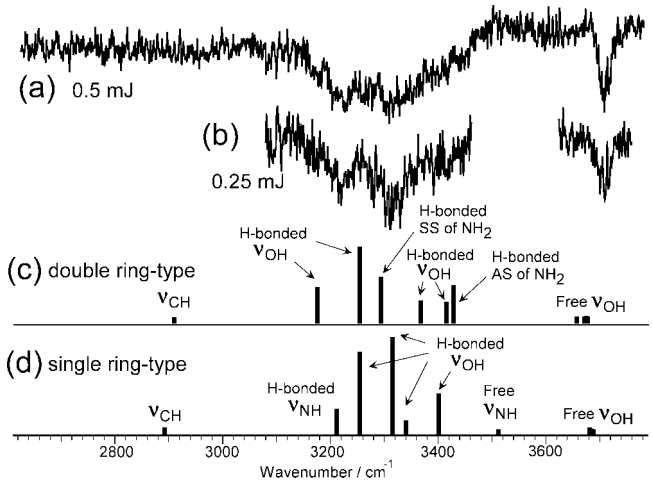

Figure 5. Infrared predissociation spectra of FA−$(H_2O)_4$ observed by monitoring the $[FA-(H_2O)_4]^+$ signal with VUV−ID−IRPDS at the IR power of (a) ∼0.5 and (b) 0.25 mJ. (c, d) Calculated spectra for the optimized structures in Figure 9 at the MP2/6-31++G** level. The calculated spectra are scaled by 0.933.

comparison of the observed spectrum with the calculated results in the next section.

IV. Discussion

IV-1. 118 nm Photoionization of Formamide−Water Clusters. In the previous section, we demonstrated that the IR spectra of neutral FA−water clusters by VUV-ID-IRPDS show clear size-dependence. To definitely determine the spectral carrier of the observed IR spectrum monitoring the $[FA-(H_2O)_n]^+$ mass channel, we need to determine the neutral precursor of each mass channel through the 118 nm photoionization.

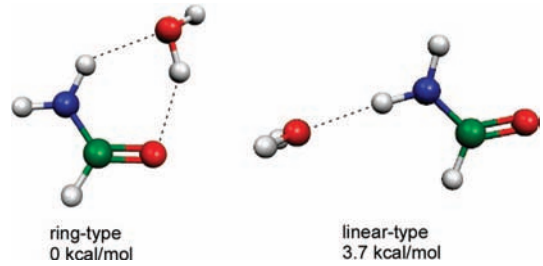

Figure 6. Optimized structures of FA−H_2O at the MP2/6-31++G** level.

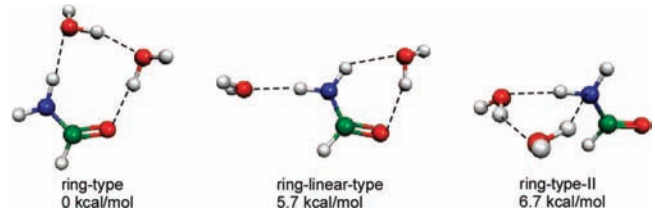

Figure 7. Optimized structures of FA−$(H_2O)_2$ at the MP2/6-31++G** level.

We first examine the spectrum obtained by monitoring the $[FA-H_2O]^+$ channel. The IR spectroscopic studies have been reported for FA−H_2O in a supersonic jet and in Ar matrix.[19–21] For the assignment of the spectral carrier of the IR spectrum in this study, it is reliable to compare it with the spectra observed by different techniques. Schermann and co-workers reported the IR spectrum of neutral FA−H_2O by the RET technique.[19,22] In this techniques, they observed the IR spectrum by monitoring the IR-induced depletion of the dipole-bound anion, $[FA-H_2O]^-$, signal produced with the RET process. Table 1 shows the observed vibrational frequencies of the IR spectra of neutral FA−H_2O obtained by the three different methods; VUV-ID-IRPDS by monitoring the $[FA-H_2O]^+$ mass channel, IR predissociation spectroscopy through the RET technique, and the matrix isolation−IR spectroscopy.[21] The spectral feature of the IR spectrum in the present study corresponds very well to that in the Ar matrix, and all the observed band frequencies agree with that observed by the RET technique. These accordances indicate the observed spectrum with VUV-ID-IRPDS by monitoring the $[FA-H_2O]^+$ mass channel is attributed to neutral FA−H_2O. In other words, $[FA-H_2O]^+$ originates from neutral FA−H_2O, which is directly ionized through the 118 nm light without the fragmentation. However, two bands at 3548 and 3454 cm^{-1} observed by Schermann and co-workers are not found in our spectrum. They reported that all the free stretching vibrational bands in their spectrum show doubling with spacing of 6−10 cm^{-1}.[19] This band splitting may be due to the coexistence of structural isomers. The bands at 3548 and 3454 cm^{-1} would also originate from structural isomers, which are produced under the different sample source condition or are emphasized by their higher electron attachment efficiencies.

In the next step, we examine the energetics in the 118 nm photoionization of the FA−H_2O system. Theoretical calculations were performed to support the above discussion. Table 2 shows the calculated results at the MP2/6-31++G** level for the adiabatic ionization energies and excess energies in the 118 nm (10.48 eV) photoionization process of FA−$(H_2O)_n$, $n = 0-2$, and the dissociation energies of $[FA-(H_2O)_n]^+$, $n = 1, 2$, to $[FA-(H_2O)_{n-1}]^+ + H_2O$. The calculated adiabatic ionization energy of FA (10.22 eV) accords with the experimental value, 10.23 eV, which is reported by Buma and co-workers with two-color photoionization and photoelectron spectroscopies.[10] The

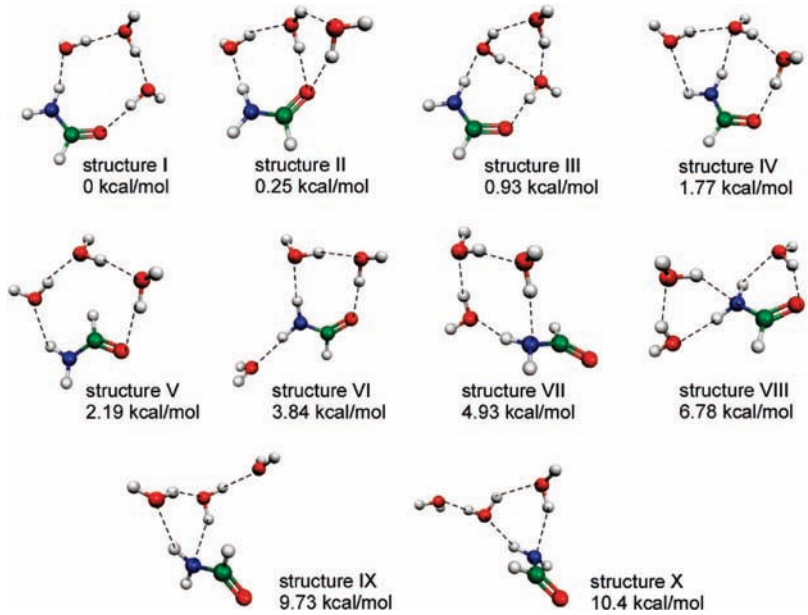

Figure 8. Optimized structures of FA−$(H_2O)_3$ at the MP2/6-31++G** level.

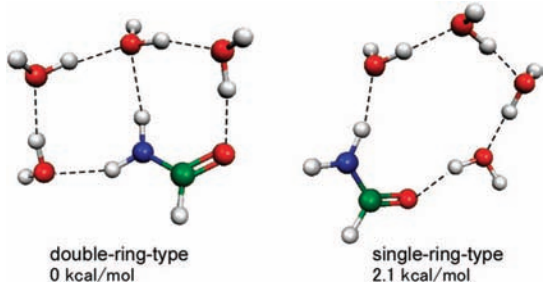

Figure 9. Optimized structures of FA−$(H_2O)_4$ at the MP2/6-31++G** level.

formation energies of the most stable ring type structures of neutral FA−H_2O and FA−$(H_2O)_2$ clusters shown in Figures 6 and 7 are used for the evaluation of the adiabatic ionization and excess energies. The adiabatic ionization and excess energies in photoionization of FA−H_2O and the dissociation energy of $[FA-H_2O]^+$ are estimated for structure V of $[FA-H_2O]^+$ in Figure 12. The cluster structures of FA−H_2O, FA−$(H_2O)_2$, and $[FA-H_2O]^+$ are discussed later. The formation energies of structures of H^+FA and $[FA-(H_2O)_2]^+$ shown in Figure 13 are adopted for the estimation of the dissociation energies and adiabatic ionization energy of FA−$(H_2O)_2$. Figure 13a shows the most stable structure of H^+FA at the MP2/6-31++G** level, which is consistent with the density functional theory (DFT) calculation of Chang and co-workers.[7] Figure 13b presents an optimized structure of $[FA-(H_2O)_2]^+$ at the MP2/6-31++G** level, which is most stable among the isomers formed by the addition of one water molecule to structure V of $[FA-H_2O]^+$. The excess energies in the photoionization processes are obtained by subtracting the calculated adiabatic ionization energies of the clusters from the 118 nm photon energy (10.48 eV). The dissociation energies of $[FA-H_2O]^+$ are the energy differences between $[FA-H_2O]^+$ and the dissociation channels, $FA^+ + H_2O$ or $H^+FA + OH$. Similarly, the dissociation energy of $[FA-(H_2O)_2]^+$ to $[FA-H_2O]^+$ is estimated by the energy difference of $[FA-(H_2O)_2]^+$ and $[FA-H_2O]^+$ (structure V) + H_2O.

The excess energy of $[FA-H_2O]^+$ in the 118 nm photoionization is smaller than the dissociation energy to the $FA^+ + H_2O$ channel, while the excess energy is enough to cause the fragmentation to $H^+FA + OH$. Therefore, $[FA-H_2O]^+$ can only dissociate into H^+FA and OH. For the dissociation channel of $[FA-(H_2O)_2]^+$ to $[FA-H_2O]^+ + H_2O$, the excess energies in the ionization process are estimated to be almost the same as the dissociation energy and the difference is only 0.09 eV. Since the intermolecular vibrational redistribution following the ionization process distributes the excess energy in the cluster cation to the dissociation coordinate, we expect a very slow dissociation rate with such a small excess energy (the RRK theory predicts the totally negligible dissociation probability ($\sim 10^{-15}$) within the observation time (~ 3 μs) of the TOF spectrometer). Thus, these theoretical evaluations also suggest that the signal intensity of the $[FA-H_2O]^+$ channel originates from neutral FA−H_2O. As discussed above, all the experimental and theoretical findings support that the observed $[FA-H_2O]^+$ signal component directly originates from FA−H_2O through the 118 nm one-photon ionization. Therefore, the IR spectrum observed with VUV-ID-IRPDS by monitoring the $[FA-H_2O]^+$ mass channel is attributed to neutral FA−H_2O.

In the IR spectra observed by monitoring $[FA-(H_2O)_n]^+$, $n = 1-4$, the spectral feature of each spectrum is different from those of others. This indicates each IR spectrum is due to a single neutral species without contamination by the cluster fragmentation in the photoionization process. The spectral carrier of the IR spectrum observed for the $[FA-H_2O]^+$ mass channel is assigned to FA−H_2O. Then, the carriers of the IR spectra observed with the $[FA-(H_2O)_n]^+$, $n = 1-4$, channels are determined to be the neutral clusters, FA−$(H_2O)_n$, $n = 1-4$, respectively. As discussed in the next section, the spectral features by monitoring $[FA-(H_2O)_n]^+$ in Figures 2–5 are well-reproduced by the calculated spectra of the most stable structures of FA−$(H_2O)_n$. $[FA-(H_2O)_n]^+$ is generated by the 118 nm photoionization of FA−$(H_2O)_n$ without the fragmentation components from larger clusters. This demonstrates the size selectivity of VUV-ID-IRPDS. No contamination of the unprotonated cluster cation mass channels from fragmentation of larger-sized clusters may be because the cluster cations mainly dissociate to produce the protonated clusters, which are expected to be energetically a more favorable fragment, as shown for the case of $[FA-H_2O]^+$ in Table 2.

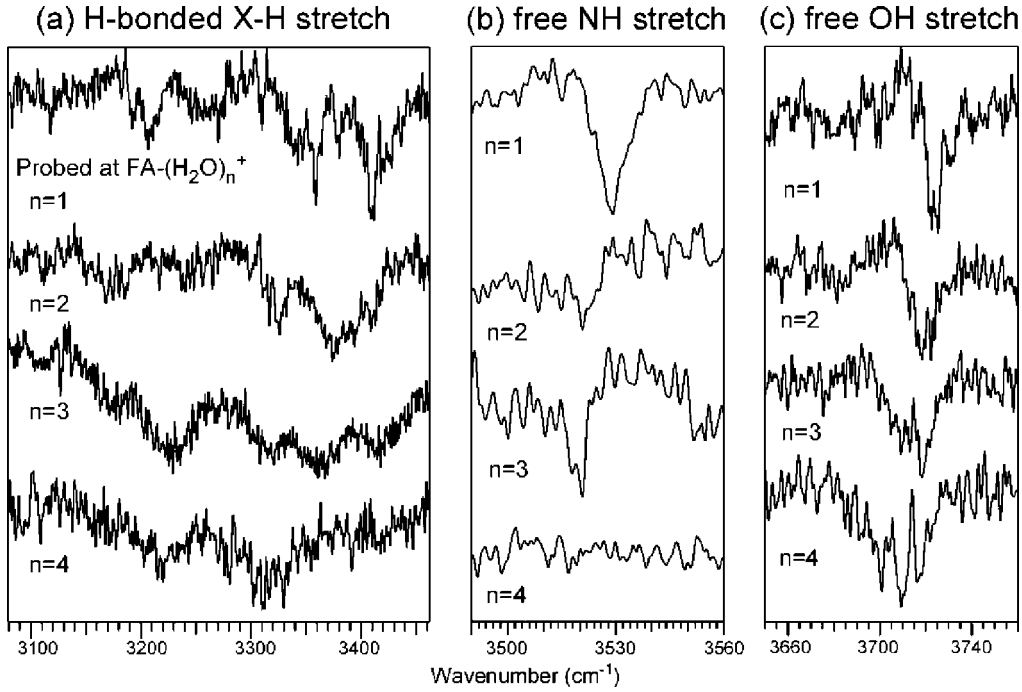

Figure 10. Expanded infrared predissociation spectra of FA−$(H_2O)_n$ (n = 1−4) in the region of (a) H-bonded NH and OH stretching, (b) free NH stretching, and (c) free OH stretching vibrational region. Spectra a and c are taken from the spectra of Figures 2–5 (spectra b) and spectra b are from the spectra of Figures 2–5 (spectra a).

IV-2. Intermolecular Structures of the Formamide−Water Clusters. Theoretical calculations for stable forms of FA−$(H_2O)_n$, n = 1−4, and their vibrational spectrum simulations were carried out to assign the spectral carriers of the observed IR spectra. The optimized structures of FA−$(H_2O)_n$, n = 1−4, at the MP2/6-31++G** level are illustrated in Figures 6–9. The harmonic frequencies based on the optimized structures were calculated and are represented by the stick spectra in Figures 2–5.

The structure of FA−H_2O has been experimentally determined by microwave spectroscopy to be the ring type structure,[18] where two H-bonds are formed between the amide group of formamide and the water moiety, as shown in Figure 6. In the Ar-matrix study,[21] the ring type structure of FA−H_2O is also the dominant form, and the linear type isomer seen in Figure 6 is found as a minor form. The ring type is more stable than the linear type by 3.7 kcal/mol at the MP2/6-31++G** level, and it is consistent with the theoretical calculations at other levels.[18,21] The simulated spectrum based on the ring type is shown in Figure 2c, and it accords with the observed spectra, which are given in Figure 2a,b. For the two bands observed at 3200−3300 cm^{-1}, we have thought they are overtone or combination modes of bending vibrations of the amino group or water. They may appear through the unharmonic coupling with the H-bonded OH and NH stretching vibrational modes.

In the observed IR spectra of FA−$(H_2O)_2$ in Figure 3a,b, three stretching vibrational bands of the H-bonded OH and NH groups appear in the region of 3100−3500 cm^{-1}, and free NH and OH stretching vibrational bands are observed at 3521 and 3720 cm^{-1}, respectively. These spectral features suggest the formation of a ring type H-bond network, where the NH group of FA and two OH groups of water molecules act as proton donors. Figure 7 illustrates the three optimized structures of FA−$(H_2O)_2$ at the MP2/6-31++G** level, and the simulated spectra of their structures are shown in Figure 3c−e. The most stable isomer is the ring type structure, where two water molecules act as a single donor and acceptor and bridge the NH and C═O groups of FA. The spectral features of the observed spectra are reproduced only by the simulated spectrum of the ring type in Figure 3c. Therefore, the structure of FA−$(H_2O)_2$ is determined to be the ring type one shown in Figure 7. This type of the intermolecular structure is similar to the most stable form of *cis-N*-benzylformamide (NBFA)−$(H_2O)_2$.[40] The formation of the ring type structure has also been reported for the gas-phase clusters with one and two water molecules of 2-pyridone,[41,42] 2-phenylacetamide (2PA),[43] and oxindole,[42] which have amide-like groups. Thus, the results of FA−$(H_2O)_n$, n = 1 and 2, strongly suggest molecules with the amide group favoring the ring type intermolecular structure with one or two water molecules, being irrespective of the presence of aromatic rings.

For the IR spectra of FA−$(H_2O)_3$ in Figure 4a,b, four H-bonded X−H (X = N, O) stretching, free NH and OH stretching vibrational bands are observed. For FA−$(H_2O)_3$, ten optimized structures shown in Figure 8 are obtained at the MP2/6-31++G** level, and the most stable five of them are almost degenerated with energy differences within 3 kcal/mol. The most stable form is the ring type shown as structure I in Figure 8, where all the three water molecules act as single donor and single acceptor in the H-bond network between the NH and C═O groups of FA. The observed vibrational spectral features are reproduced only by the simulated spectrum for structure I in Figure 8 among ten structural isomers. It clearly shows that FA−$(H_2O)_3$ forms the ring type intermolecular form of structure I. The observed peak widths of the H-bonded NH and OH stretching vibrations are very broad, and therefore, there remains the probability of the contribution of other minor isomers.

The IR spectra and theoretical calculations of hydrated clusters with three water molecules have been reported for several molecules having an amide group, such as NBFA and 2PA.[40,43] The energy differences of their ring type isomer similar to structure I and triangular water type structure III of FA−$(H_2O)_3$ were reported to be less than 3 kcal/mol.[40,43] The cis-form of NBFA−$(H_2O)_3$ prefers the triangular water type because of the interaction between the H-bond network and the

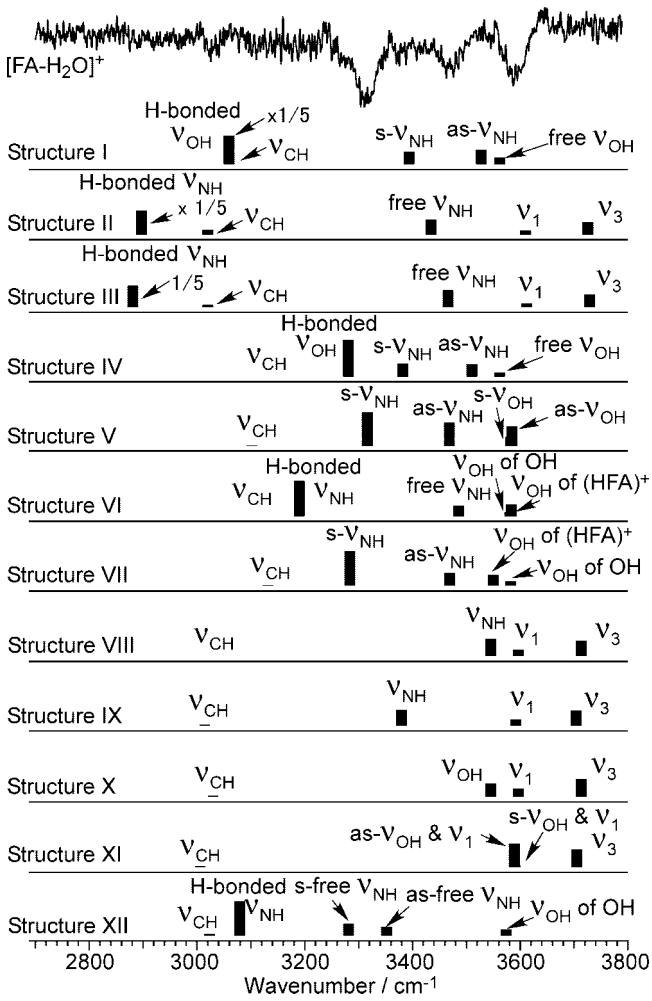

Figure 11. Infrared predissociation spectra of $[FA-H_2O]^+$ observed with IR predissociation spectroscopy of VUV−pumped ion (IRPDS−VUV−PI) and calculated spectra for the optimized structures of $[FA-H_2O]^+$ at the MP2/6-31++G** level shown in Figure 12. The calculated spectra are scaled by 0.943.

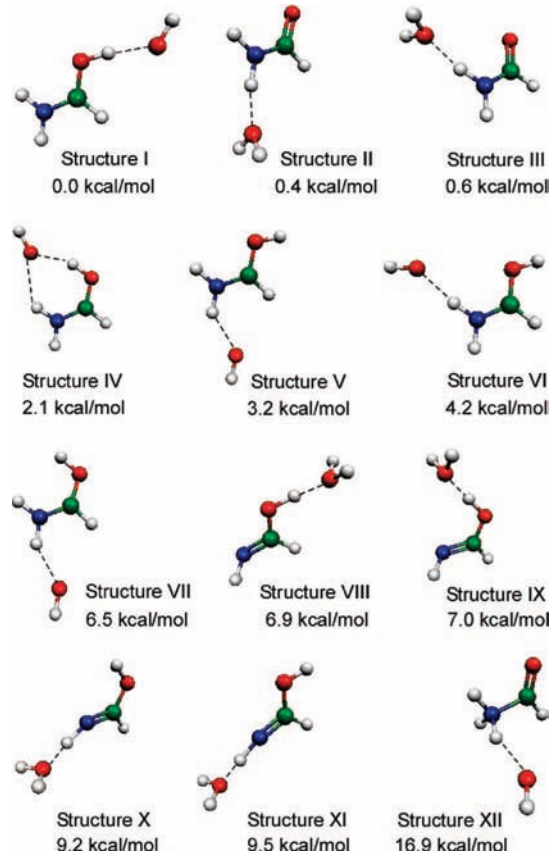

Figure 12. Optimized structures of $[FA-H_2O]^+$ at the MP2/6-31++G** level.

π-electrons of the phenyl group. On the other hand, $2PA-(H_2O)_3$ forms the ring type intermolecular structure similar to structure I of $FA-(H_2O)_3$. Therefore, the amide group and three water molecules would favor the formation of the H-bond network such as that of structure I in Figure 8 without perturbations from other substituted groups.

The free NH stretching vibration does not appear in the IR spectra of $FA-(H_2O)_4$ in Figure 5a,b. Figure 9 shows the optimized structures of $FA-(H_2O)_4$ at the MP2/6-31++G** level, and the double ring type form is estimated to be more stable by 2.1 kcal/mol than the single ring type. In the double-ring type, the H-bond network with water molecules involves the two NH bonds of the amino group and the C=O group of FA as shown in the figure. The single ring type structure has a simple H-bond network chain of four water molecules between one of the N−H bonds and the C=O group of FA. The H-bond networks of both structures are formed with a small distortion of each H-bond, which has the intermolecular H···X (X = O, N) distance of ~1.8 Å and the O(N)−H···O angle of ~170°. Therefore, the difference of the formation energies might be due to the difference of the numbers of H-bonds formed between two isomers. In comparison between the observed and simulated spectra, the spectral feature in the H-bonded X−H (X = O, N) stretching vibrational region is heavily complicated; therefore this region is not informative. The key feature to determine the structure is that the observed IR spectrum shows no free NH stretching vibration while the spectra of $n = 1-3$ exhibit the clear free NH stretching vibrational bands. This feature of the IR spectrum of $n = 4$ means both of the two NH bonds of the amino group of FA act as the H-bond donor. This is clear evidence for the double ring type structure. The vibrational calculation of the double ring type structure in Figure 5c represents no free NH stretching vibration, as easily expected. Therefore, we conclude that $FA-(H_2O)_4$ forms the double ring type structure in Figure 9. This implies that the first hydrated shell around the H-bonding sites of FA is completed with four water molecules.

IV-3. Intracluster Hydrogen Transfer of Formamide−Water Cluster Induced by Ionization. In the IR spectrum of $[FA-H_2O]^+$, no band appears in the region of 3650−3790 cm^{-1}, which corresponds to the characteristic ν_3 or free OH stretching vibration of the neutral water moiety. This fact suggests that the water moiety no longer holds its neutral form in $[FA-H_2O]^+$. For the more detailed analysis of the structure of $[FA-H_2O]^+$, theoretical calculations at the MP2 level were carried out for the structures and vibrational frequencies. The twelve optimized structures of $[FA-H_2O]^+$ are obtained at the MP2/6-31++G** level calculations. The structures and IR spectral simulations are presented in Figures 12 and 11, respectively. Structures I and IV−VII have the $(H-FA)^+-OH$ type H-bonded compositions, where a hydrogen atom of the water is transferred to the carbonyl oxygen of FA^+. Structures II and III are regarded as H-bonded clusters of FA^+ and neutral water. Structures VIII−XI are the cluster cations of water and formimide cation (FI^+), which is a tautomer of FA^+. Structures VIII−XI of FI^+-H_2O tend to be less stable compared to

TABLE 1: Vibrational Frequencies (cm^{-1}) Observed by Monitoring $[FA-H_2O]^+$ Signal with VUV-ID-IRPDS in This Study, by Schermann and Co-workers with monitoring of the $(FA-H_2O)^-$ Ion Signal Produced with the Rydberg Electron-Transfer (RET) Technique and by Ar-Matrix Spectroscopy

	this study	RET[a]	Ar matrix [b]
free OH stretch	3724	3727 3548	3707
free NH stretch	3529	∼3528 [c] 3454	3522
H-bonded OH stretch	3410	3410	3430
H-bonded NH stretch	3359	*d*	3391
CH stretch	2873	2874	2887

[a] Reference 19. [b] Reference 21. [c] This frequency is estimated from the spectrum in ref 19. [d] This region was not observed.

FA^+-H_2O and $(H-FA)^+-OH$ of structures I−VII. Structure XII is the highest energy conformer of the $(H-FA)^+-OH$ composition, where a hydrogen atom is transferred from the water moiety to the amino nitrogen atom of FA^+. Chang and co-workers have shown the O-protonation form of protonated formamide is more stable than the N-protonation form by DFT calculation at the B3LYP/6-31+G* level.[7,8] It is, consequently, considered that the hydrogen (H) transfer to the amino nitrogen atom of FA^+ is energetically unfavorable.

In the vibrational spectral simulations, the intense stretching bands of the free OH groups of water are expected in the region of 3700−3750 cm^{-1} for structures II, III, and VIII−XI, which contain the neutral water moiety. On the other hand, no vibrational band is predicted in the higher region than 3600 cm^{-1} for the H-transferred forms: structures I, IV−VII, and XI. No feature is experimentally observed in the free OH vibrational region. Thus, the experimental finding also supports a hydrogen atom of the water moiety being transferred to FA^+.

Among the simulated spectra of the potential candidates, structures I and IV−VII, the spectra of structures IV−VII are similar to one another and also resemble the observed spectrum, while the intense H-bonded OH stretching vibration of structure I does not appear in the observed spectrum. The three intense bands in the observed spectrum are most properly simulated by the calculated spectrum of structure V. The calculated spectral features of structures IV and VII also fit the observed spectrum, if their two highest frequency bands are overlapped in the observed spectrum. Structures V−VII have the same type of intermolecular structure, where the H-bond is formed between the amino hydrogen of FA^+ and the oxygen of the OH radical. The unique structure difference among them is the orientation angle of the OH group of FA^+ around the C−O axis, though the OH group of FA^+ is not directly related to the intermolecular interaction in these isomers. In the intermolecular structure of structure IV, both the OH and NH groups of FA^+ act as the H-bond donor of the interaction between FA^+ and OH.

To discuss an intermolecular structure based on its vibrational spectral feature, it is important to check the dependency of calculated spectra on the basis set functions. Vibrational simulations with various levels of basis sets are carried out for structures IV and V, which have different types of intermolecular structures but similar vibrational features at the MP2/6-31++G** level. Comparisons of (a) the observed and calculated spectra with several basis sets of structures (b) IV and (c) V are shown in Figure 14. In all the MP2 geometry optimizations, structure IV is more stable by 1−2 kcal/mol than structure V. For open-shell cluster cations, however, such an energy difference would be too small to rely on, because of the strong dependency of an isomeric energy difference on the calculation levels for open-shell systems.[36] In the vibrational simulation of structure IV, the frequency difference of the highest two bands is calculated to be 48−113 cm^{-1} depending on the basis sets, while the half-width at half-maximum of the observed band at 3592 cm^{-1} is only ∼40 cm^{-1}. The expected frequency spacing is large enough to be seen in the spectral feature, if the structure IV isomer contributes to the observed spectrum. And, also, the calculated CH stretching vibrational frequencies of structure IV are largely mismatched with the observed ones (3028 cm^{-1}). On the other hand, the observed spectral features are well-reproduced by the simulated spectra of structure V with all the basis sets, except for the one at MP2/aug-cc-pVDZ, where the calculated frequency of the CH stretching vibration differs by ∼40 cm^{-1} from the other levels. Therefore, it can be concluded that $[FA-H_2O]^+$ forms the H-transferred type structure such as structure V.

The excess energy in the 118 nm photoionization of $FA-H_2O$ is not negligibly small, as listed in Table 2. Therefore, it may be possible that the cluster becomes flexible at the present excess energy, and several structural isomers such as structures IV−VII coexist through the isomerization due to the rotations of the amino and hydroxyl groups of $(HFA)^+$.

The H-transferred structure of $[FA-H_2O]^+$ is thought to be formed through a transfer reaction of a hydrogen atom or a proton of water to FA^+ upon ionization. In the 118 nm one-photon ionization of $FA-H_2O$, the FA moiety is first vertically ionized in the cluster, because of the higher ionization energy of water than the one-photon energy of the 118 nm light. Therefore, the positive charge is initially localized in the FA moiety. To identify which transfer reaction (hydrogen or proton) is responsible for the formation of the H-transferred structure, it is essential to exam the charge distribution of the product ion, $[FA-H_2O]^+$. Figure 15 shows atomic charges of structure V of $[FA-H_2O]^+$, which are obtained by the natural bond orbital (NBO) and Mulliken charge analyses.[37] As shown in the figure, the positive charge is mostly localized on the $(HFA)^+$ moiety, while the total charge of the OH radical moiety is almost negligible. These results imply that $[FA-H_2O]^+$ of structure V is formed by the extraction of a neutral hydrogen atom of water

TABLE 2: Calculated and Experimental Adiabatic Ionization Energies, Excess Energies in 118 nm (10.48 eV) Photoionization, and Dissociation Energies of $FA-(H_2O)_n$, $n = 0-2$ (All Units in electronvolts)

	adiabatic ionization energy			
	calcd[a]	exptl[b]	excess energy[a]	dissociation energy[a]
FA^+	10.22	10.23	0.26	
$[FA-H_2O]^+$ (structure V)	9.85		0.63	0.54 $[FA-H_2O]^+ \rightarrow H^+FA + OH$ 0.82 $[FA-H_2O]^+ \rightarrow FA^+ + H_2O$
$[FA-(H_2O)_2]^+$	9.38		1.10	1.01 $[FA-(H_2O)_2]^+ \rightarrow [FA-H_2O]^+$ (structure V) + H_2O

[a] MP2/6-31++G**. [b] Two-color photoionization.[10]

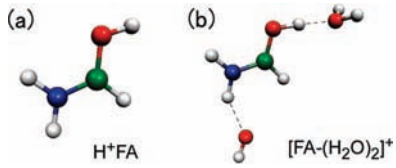

Figure 13. Optimized structures of (a) H^+FA and (b) $[FA-(H_2O)_2]^+$ at the MP2/6-31++G** level.

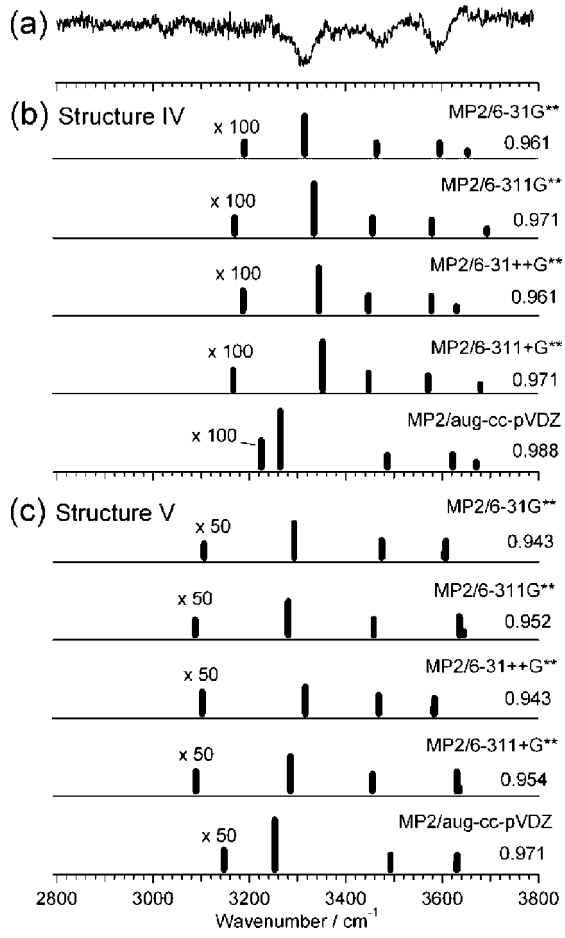

Figure 14. Comparisons of (a) the observed infrared spectrum and calculated spectra for (b) structure IV and (c) structure V of $[FA-H_2O]^+$ by the MP2 calculations with the various basis sets. The observed infrared spectrum is reproduced from Figure 11. Scaling factors for the simulated spectra are chosen to fit the frequencies of the calculated three intense modes with those of the observed three intense peaks.

to FA^+ following the photoionization of FA in the cluster. These steps are schematically represented as follows.

$$FA-H_2O \xrightarrow[\text{18 nm photoionization}]{} FA^+-H_2O \xrightarrow[\text{H-transfer}]{} (HFA)^+-OH \quad (1)$$

We have previously found that the ammonia dimer cation, $(NH_3)_2^+$, forms the H-transferred structure, which is the cluster cation of NH_4^+ and NH_2 radical.[36] Thus, H-transfer reactions tend to occur in the photoionization of the clusters of protic molecules. Such H-transferred structures of the clusters of protic molecules may be regarded as the precursor of their protonated cluster generation.

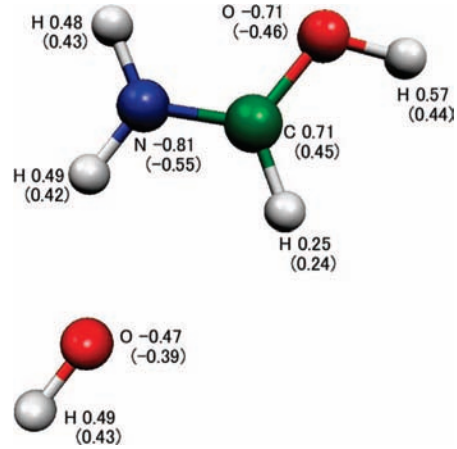

Figure 15. Calculated atomic charges of the NBO and Mulliken population analyses at the MP2/6-31++G** level for structure V of $[FA-H_2O]^+$ shown in Figure 12. The Mulliken charges are in parentheses.

V. Conclusions

In this study, the structures of neutral $FA-(H_2O)_n$, $n = 1-4$, were determined by the vibrational spectra observed with VUV-ID-IRPDS and by the theoretical calculations at the MP2/6-31++G** level. In the stepwise hydration structures of FA, $FA-(H_2O)_n$ forms the ring type structures at $n = 1-3$, where water molecules act as single donor and acceptor in the single ring type H-bond network between the amino and carbonyl groups of FA. The double ring type structure was suggested for $FA-(H_2O)_4$. In this structure, two ring type H-bond networks are formed among the carbonyl oxygen and amino hydrogens, being linked by a water molecule which acts as a single donor and double acceptor.

The spectroscopic principle of VUV-ID-IRPDS was demonstrated by the observation of the IR spectra of the size-selected formamide−water clusters, which have no suitable chromophore for the conventional IR−UV double resonance techniques. Thus, VUV-ID-IRPDS is quite advantageous to IR spectroscopy of size-selected neutral molecular clusters irrespective of a suitable UV chromophore.

The structure of $[FA-H_2O]^+$ was also investigated by the observation of the IR spectrum with IRPDS-VUV-PI and the theoretical calculations at the MP2 level with the various basis sets. $[FA-H_2O]^+$ forms the H-transferred structure, $(HFA)^+-OH$, where the hydrogen atom of the water moiety is transferred to the FA^+ moiety.

In mass spectrometric studies of biomolecules with matrix assisted laser desorption/ionization (MALDI) technique, their protonated species are generally formed. The generation mechanism of protonated ions has not been fully understood, because the ion can be produced in any steps of the MALDI process. Formamide is the most simple model of polypeptide, and it has been clarified in this study that its cation subtracts a hydrogen atom from the surrounding solvent molecule. This may be a helpful finding to understand the MALDI mechanism in the molecular level.

Acknowledgment. We thank Dr. T. Maeyama and Mr. K. Ohta for their helpful discussions. This work was supported by the Ogasawara Foundation for the Promotion of Science & Engineering, the Grant-in-Aid for specially promoted research (Grant No. 16002006) and Priority Areas "Molecular Science for Supra Functional Systems " (Grant No. 477) from the Ministry of Education, Culture, Sports, Science and

Technology (MEXT), Japan, and a Grant in Aid for Scientific Research Projects Nos. 19205001 and 18656009 from JSPS, Japan.

References and Notes

(1) Zwier, T. S. *Annu. Rev. Phys. Chem.* **1996**, *47*, 205.
(2) Scherer, J. J.; Paul, J. B.; O'Keefe, A.; Saykally, R. J. *Chem. Rev.* **1997**, *97*, 25.
(3) Ebata, T.; Fujii, A.; Mikami, N. *Int. Rev. Phys. Chem.* **1998**, *17*, 331.
(4) Buck, U.; Huisken, F. *Chem. Rev.* **2000**, *100*, 3863.
(5) Brutschy, B. *Chem. Rev.* **2000**, *100*, 3891.
(6) Dessent, C. E. H.; Müller-Dethlefs, K. *Chem. Rev.* **2000**, *100*, 3999.
(7) Wu, C.-C.; Jiang, J. C.; Hahndorf, I.; Chaudhuri, C.; Lee, Y. T.; Chang, H.-C. *J. Phys. Chem. A* **2000**, *104*, 9556.
(8) Chaudhuri, C.; Jiang, J. C.; Wu, C.-C.; Wang, X.; Chang, H.-C. *J. Phys. Chem. A* **2001**, *105*, 8906.
(9) Maeyama, T.; Negishi, Y.; Tsukuda, T.; Yagi, I.; Mikami, N. *Phys. Chem. Chem. Phys.* **2006**, *8*, 827.
(10) ter Steege, D. H. A.; Lagrost, C.; Buma, W. J.; Leigh, D. A.; Zerbetto, F. *J. Chem. Phys.* **2002**, *117*, 8270.
(11) Lin, H.-Y.; Ridge, D. P.; Uggerud, E.; Vulpius, T. *J. Am. Chem. Soc.* **1994**, *116*, 2996.
(12) Antonczak, S.; Ruiz-López, M. F.; Rivail, J. L. *J. Am. Chem. Soc.* **1994**, *116*, 3912.
(13) Ou, M.-C.; Chu, S.-Y. *J. Phys. Chem.* **1995**, *99*, 556.
(14) Tortajada, J.; Leon, E.; Morizur, J. -P.; Luna, A.; Mó, O.; Yáñez, M. *J. Phys. Chem.* **1995**, *99*, 13890.
(15) Pranata, J.; Davis, G. D. *J. Phys. Chem.* **1995**, *99*, 14340.
(16) Luna, A.; Amekraz, B.; Torajada, J.; Morizur, J. P.; Alcamí, Mó, O.; Yáñez, M. *J. Am. Chem. Soc.* **1998**, *120*, 5411.
(17) Kamitakahara, A.; Pranata, J. *J. Mol. Struct. (Theochem)* **1998**, *429*, 61.
(18) Lovas, F. J.; Suenram, R. D.; Fraser, G. T. *J. Chem. Phys.* **1988**, *88*, 722.
(19) Lucas, B.; Lecomte, F.; Reimann, B.; Barth, H.-D.; Grégoire, G.; Bouteiller, Y.; Schermann, J.-P.; Desfrançois, C.;. *Phys. Chem. Chem. Phys.* **2004**, *6*, 2600.
(20) Lucas, B.; Grégoire, G.; Lecomte, F.; Reimann, B.; Schermann, J.-P.; Desfrançois, C. *Mol. Phys.* **2005**, *103*, 1497.
(21) Engdahl, A.; Nelander, B.; Åstrand, P.-O. *J. Chem. Phys.* **1993**, *99*, 4894.
(22) Seydou, M.; Modelli, A.; Lucas, B.; Konate, K.; Desfrançois, C.; Schermann, J.-P.;. *Eur. Phys. J. D* **2005**, *35*, 199.
(23) (a) Asmis, K. R.; Pivonka, N. L.; Santambrogio, G.; Brümmer, M.; Kaposta, C.; Neumark, D. M.; Wöste, L. *Science* **2003**, *299*, 1375. (b) Miyazaki, M.; Fujii, A.; Ebata, T.; Mikami, N. *Science* **2004**, *304*, 1134. (c) Shin, J.-W.; Hammer, N. I.; Diken, E. G.; Johnson, M. A.; Walters, R. S.; Jaeger, T. D.; Duncan, M. A.; Christie, R. A.; Jordan, K. D. *Science* **2004**, *304*, 1137. (d) Headrick, J. M.; Diken, E. G.; Walters, R. S.; Hammer, N. I.; Christie, R. A.; Cui, J.; Myshakin, E. M.; Duncan, M. A.; Johnson, M. A.; Jordan, K. D. *Science* **2005**, *308*, 1765. (e) Wu, C.-C.; Lin, C.-K.; Lee, Y. T.; Chang, H.-C.; Jiang, J.-C.; Kuo, J.-L.; Klein, M. L. *J. Chem. Phys.* **2005**, *122*, 074315. (f) Mizuse, K.; Fujii, A.; Mikami, N. *J. Chem. Phys.* **2007**, *126*, 231101.
(24) (a) Chang, H.-C.; Jiang, J.-C.; Lin, S. H.; Lee, Y. T.; Chang, H.-C. *J.Phys. Chem. A* **1999**, *103*, 2941. (b) Chang, H.-C.; Jiang, J.-C.; Chang, H.-C.; Wang, L. R.; Lee, Y. T. *Isr. J. Chem.* **1999**, *39*, 231. (c) Solca, N.; Dopfer, O. *J. Am. Chem. Soc.* **2004**, *126*, 9520. (d) Fujii, A.; Enomoto, S.; Miyazaki, M.; Mikami, N. *J. Phys. Chem. A* **2005**, *109*, 138. (e) Suhara, K.; Fujii, A.; Mizuse, K.; Mikami, N.; Kuo, J.-L. *J. Chem. Phys.* **2007**, *126*, 194306.
(25) (a) Price, J. M.; Crofton, M. W.; Lee, Y. T. *J. Phys. Chem.* **1991**, *95*, 2182. (b) Tono, K.; Fukazawa, K.; Tada, M.; Fukushima, N.; Tsukiyama, K. *Chem. Phys. Lett.* **2007**, *442*, 206.
(26) (a) Inokuchi, Y.; Nishi, N. *J. Phys. Chem. A* **2002**, *106*, 4529. (b) Inokuchi, Y.; Nishi, N. *J. Phys. Chem. A* **2003**, *107*, 11319. (c) Kong, X.; Tsai, I.-A.; Sabu, S.; Han, C.-C.; Lee, Y. T.; Chang, H.-C.; Tu, S.-Y.; Kung, A. H.; Wu, C.-C. *Angew. Chem.* **2006**, *118*, 4236. (d) Aleese, L. M.; Simon, A.; McMahon, T. B.; Ortega, J.-M.; Scuderi, D.; Lemaire, J.; Maître, P. *Int. J. Mass Spectrom.* **2006**, *249−250*, 14. (e) Hu, Y. J.; Fu, H. B.; Bernstein, E. R. *J. Chem. Phys.* **2006**, *125*, 184309.
(27) (a) Wei, S.; Tzeng, W. B.; Castleman, A. W., Jr *J. Chem. Phys.* **1990**, *92*, 332. (b) Wei, S.; Tzeng, W. B.; Castleman, A. W. J., Jr. *Chem. Phys.* **1990**, *93*, 2506. (c) Misaizu, F.; Houston, P. L.; Nishi, N.; Shinohara, H.; Kondow, T.; Kinoshita, M. *J. Chem. Phys.* **1993**, *98*, 336.
(28) (a) Shinohara, H.; Nishi, N.; Washida, N. *J. Chem. Phys.* **1985**, *83*, 1939. (b) Shinohara, H.; Nishi, N.; Washida, N. *J. Chem. Phys.* **1986**, *84*, 5561. (c) Shi, Y. J.; Consta, S.; Das, A. K.; Mallik, B.; Lacey, D.; Lipson, R. H. *J. Chem. Phys.* **2002**, *116*, 6990. (d) Dong, F.; Heinbuch, S.; Rocca, J. J.; Bernstein, E. R. *J. Chem. Phys.* **2006**, *124*, 224319.
(29) (a) Buzza, S. A.; Wei, S.; Purnell, J.; Castleman, A. W., Jr. *J. Chem. Phys.* **1995**, *102*, 4832. (b) Witt, M.; Grutzmacher, H. F. *Int. J. Mass Spectrom.* **1997**, *165*, 49.
(30) Yang, S.; Brereton, S. M.; Nandhra, S.; Ellis, A. M.; Shang, B.; Yuan, L.-F.; Yang, J. *J. Chem. Phys.* **2007**, *127*, 134303.
(31) Woo, H. K.; Wang, P.; Lau, K.-C.; Xing, X.; Chang, C.; Ng, C. Y. *J. Chem. Phys.* **2003**, *119*, 9333.
(32) Bahng, M.-K.; Xing, X.; Baek, S. J.; Ng, C. Y. *J. Chem. Phys.* **2005**, *123*, 84311.
(33) Fu, H. B.; Hu, Y. J.; Bernstein, E. R. *J. Chem. Phys.* **2006**, *124*, 24302.
(34) Matsuda, Y.; Mori, M.; Masaki, M.; Fujii, A.; Mikami, N. *Chem. Phys. Lett.* **2006**, *422*, 378.
(35) Matsuda, Y.; Hachiya, M.; Fujii, A.; Mikami, N. *Chem. Phys. Lett.* **2007**, *442*, 217.
(36) Matsuda, Y.; Mori, M.; Masaki, M.; Fujii, A.; Mikami, N. *J. Chem. Phys.* **2006**, *125*, 164320.
(37) Frisch, M. J.; Trucks, G. W.; Schlegel, H. B.; Scuseria, G. E.; Robb, M. A.; Cheeseman, J. R.; Montgomery, J. A., Jr.; Vreven, T., Kudin, K. N.; Burant, J. C.; Millam, J. M.; Iyengar, S. S.; Tomasi, J.; Barone, V.; Mennucci, B.; Cossi, M.; Scalmani, G.; Rega, N.; Petersson, G. A.; Nakatsuji, H.; Hada, M.; Ehara, M.; Toyota, K.; Fukuda, R.; Hasegawa, J.; Ishida, M.; Nakajima, T.; Honda, Y.; Kitao, O.; Nakai, H.; Klene, M.; Li, X.; Knox, J. E.; Hratchian, H. P.; Cross, J. B.; Bakken, V.; Adamo, C.; Jaramillo, J.; Gomperts, R.; Stratmann, R. E.; Yazyev, O.; Austin, A. J.; Cammi, R.; Pomelli, C.; Ochterski, J. W.; Ayala, P. Y.; Morokuma, K.; Voth, G. A.; Salvador, P.; Dannenberg, J. J.; Zakrzewski, V. G.; Dapprich, S.; Daniels, A. D.; Strain, M. C.; Farkas, O.; Malick, D. K.; Rabuck, A. D.; Raghavachari, K.; Foresman, J. B.; Ortiz, J. V.; Cui, Q.; Baboul, A. G.; Clifford, S.; Cioslowski, J.; Stefanov, B. B.; Liu, G.; Liashenko, A.; Piskorz, P.; Komaromi, I.; Martin, R. L.; Fox, D. J.; Keith, T.; Al-Laham, M. A.; Peng, C. Y.; Nanayakkara, A.; Challacombe, M.; Gill, P. M. W.; Johnson, B.; Chen, W.; Wong, M. W.; Gonzalez, C.; Pople, J. A. *Gaussian 03*, Revision C.02; Gaussian: Wallingford, CT, 2004.
(38) Flukiger, P.; Luthi, H. P.; Portmann, S.; Weber, J. *Molekel 4.0*; Swiss Center for Scientific Computing: Manno, Switzerland, 2000.
(39) Karlsson, L.; Mattson, L.; Jadrny, R.; Albridge, R. G.; Pinchas, S.; Bergmark, T.; Siegbahn, K. *J. Chem. Phys.* **1975**, *62*, 4745.
(40) Robertson, E. G.; Hockridge, M. R.; Jelfs, P.; Simons, J. P. *J. Phys. Chem. A* **2000**, *104*, 11714.
(41) (a) Matsuda, Y.; Ebata, T.; Mikami, N. *J. Chem. Phys.* **1999**, *110*, 8397. (b) Matsuda, Y.; Ebata, T.; Mikami, N. *J. Chem. Phys.* **2000**, *113*, 573. (c) Matsuda, Y.; Ebata, T.; Mikami, N. *J. Phys. Chem. A* **2001**, *105*, 3480.
(42) Zwier, T. S. *J. Phys. Chem. A* **2001**, *105*, 8827.
(43) Robertson, E. G.; Hockridge, M. R.; Jelfs, P.; Simons, J. P. *Phys. Chem. Chem. Phys.* **2001**, *3*, 786.

JP800743B